

Kalman Filter as Tool for the Real-time Detection of Fast Displacements by the Use of Low-cost GPS Receivers

Paolo Dabove and Ambrogio Maria Manzino

Environment, Land and Infrastructure Department, Politecnico di Torino, Corso Duca degli Abruzzi 24, Turin, Italy

Keywords: Landslide Monitoring, GNSS NRTK Positioning, Mass-market Receivers, Kalman Filter, Accuracy.

Abstract: In this paper the problem of landslide monitoring and deformation analysis using the Kalman filter and results obtained from a GPS mass-market receiver in real-time is addressed. Landslide monitoring and deformation analysis are relevant aspects about the safety of human life in any terrain where landslides can impact human activity. It is therefore necessary to monitor these effects in order to detect and prevent these risks. Very often, most of this type of monitoring is carried out by using traditional topographic instruments (e.g. total stations) or satellite techniques such as GNSS receivers, and many experiments were carried out considering these types of mass-market instruments. In this context it is fundamental to detect whether or not deformation exists, in order to predict future displacement. Filtering means are essential to process the diverse noisy measurements (especially if low cost sensors are considered) and estimate the parameters of interest. In this paper a particular version of Kalman Filter is considered in order to understand if there are any displacements from a statistical point of view in real time. The tests, the algorithm and results are herein reported.

1 INTRODUCTION

Deformation monitoring is the act of ordinary and continuous observation of such variations that are referred to as “deformation” (Sedlak and Jecny, 2004; Chrzanowski et al., 1986).

Considering the types of network, deformation survey techniques are classified as Absolute Deformation Monitoring (some reference points located in the area surrounding the object of interest, i.e. dam, bridge, etc.) and Relative Deformation Monitoring (where the reference points are located in the structure and both the object and reference points are subject to displacement) (Aharizad et al., 2012; USACE, 2002). Methods of deformation monitoring have changed considerably in principle over the past few decades as newer data sources have come to be used. In sparsely vegetated terrain, landslides are routinely detected and mapped by a combination of the interpretation of airphotos or multispectral digital imagery and selective ground verification (Benoit et al., 2014). However, it is quite difficult to use these methods in rugged terrain covered with dense vegetation. Also, landslide inventory mapping studies typically focus on outlining boundaries and neglect

the wealth of information revealed by internal deformation features (Cruden, 1991).

With regard to deformation analysis, it is possible to consider two main categories (Szostak-Chrzanowski et al., 2005): geometrical analysis, which detects the location and the magnitude of the deformation, and physical interpretation, which determines the relationship between the deformation and its causes. In this context, there are four types of models that allow the analysis of deformation (Welsch and Heunecke, 2001; Aharizad et al., 2012; Brückl et al., 2013) These are the static, kinematic, dynamic and congruence models.

This paper focuses attention on the second type of model. Kinematic models describe deformation as a function of time, including velocity and acceleration. It is also possible to classify data processing techniques into two main groups. The first consists of robust methods, such as Iterative Weighted Similarity Transformation (IWST) and tests (e.g. Chow test, Chow, 1960; Bellone et al., 2016), while the second one is composed of non-robust methods, e.g. Kalman Filter (Li and Kuhlmann, 2008; Tasci, 2010; Simon, 2001; Güral, 1999; Acar et al, 2004; Masiero et al, 2013). In this study attention is focused on these last methods, and especially on the Kalman Filter, in

order to perform a 3-D deformation analysis using a low-cost single-frequency GPS data in real-time.

Some previous studies have also investigated the accuracy obtainable with geodetic receivers and antennas (Li and Kuhlmann, 2010 and 2012) while some of them have also considered the mass-market ones for landslide monitoring (Janssen and Rizos 2003; Squarzoni et al., 2005; Heunecke et al., 2011). Those studies used both post-processing (Cina and Piras, 2014) and real-time (Bellone et al., 2016) approaches in order to analyze the various types of landslide phenomena. In both cases, the most notable feature of these instruments is that they provide centimeter or sub-centimeter accuracy in real time when phase ambiguity is adjusted (Manzino and Dabove, 2013). This is also observed in considering different GNSS positioning techniques (Othman et al. 2011a; Othman et al. 2011b) such as static (Brunner et al. 2007), rapid-static (Hastaoglu and Sanli 2011), and real-time kinematic (RTK - Wang 2011) positioning.

A practical case study will show the reliability of the results obtained through the Kalman filter as a statistical tool to detect and predict displacements in real-time. A brief comparison of the results obtained by this method and those obtained with the modified Chow test (Bellone et al., 2016) will conclude this work.

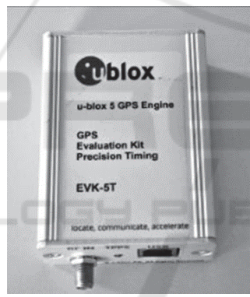
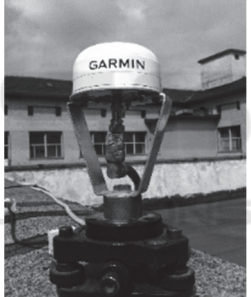
2 GNSS INSTRUMENTS CONSIDERED FOR LANDSLIDES ANALYSIS

Nowadays, many types of GNSS instruments are available functioning in a variety of frequencies, constellations and accuracies obtainable both in real-time and post-processing (Dabove et al., 2014; Dabove and Manzino, 2014). As previously stated, GPS/GNSS instruments are very often used for landslides monitoring (Eyo Etim et al., 2014) and are frequently coupled with other instruments such as theodolite, Electronic Distance Measurement (EDM) (Günther et al., 2008), levels, total station (Rizzo, 2002), inclinometers (Calcaterra et al., 2012), and wire extensometers (Bertachini et al. 2009; Coe et al. 2003; Gili et al., 2000; Malet et al., 2002; Moss, 2000; Tagliavini et al., 2007).

In other studies GPS instruments were integrated with other surveying techniques, such as terrestrial laser scanning, Synthetic Aperture Radar (SAR) interferometry (Peyret et al., 2008; Rott and Nagler 2006), and photogrammetry (Mora et al., 2003), to

investigate landslide phenomena (Wang and Soler, 2012). Some studies have also investigated the accuracy of low-cost single-frequency GPS receivers for landslide monitoring (Janssen and Rizos, 2003; Squarzoni et al. 2005) both in post-processing, (Cina and Piras, 2014), and in real-time approaches (Bellone et al., 2016) in order to analyze various types of landslide phenomena (landslides with low constant velocity or with an unexpected and sudden displacement). Considering the first approach, raw GNSS measurements are acquired and post-processed in a single- or multi-base solution with one or more GNSS permanent stations or Virtual Rinx while, considering the second one, differential corrections provided by CORSs networks are used to determine the rover position in real-time. In this paper we focus our attention only on this last approach, analysing displacements in real-time.

Table 1: Characteristics of GPS receiver and antenna.

Receiver: uBlox LEA EVK-5T Evaluation kit	Antenna: Garmin GA38 GPS& Glonass L1
	
Constellation: GPS (50 channels)	Constellation: GPS + GLONASS
Observations: C/A L1, Doppler, S/N	Gain 27 dB on the average
Cost: about 250 €	Cost: about 50 €

The employment of mass-market receivers and antennas is due to the fact that there is a high probability to lose these instruments if an unexpected displacement occurs: in this context, the amount of cost is less than 1000 € for each receiver + antenna that is an order of magnitude less than geodetic instruments. For this study, an u-blox EVK-5T receiver (Table 1- left) with an external antenna (Garmin GA38, Table 1 - right) was used. This receiver has a cost of about 350 € (including a patch antenna) while the cost of the Garmin antenna is about 50 €. One of the features of this receiver is that it is able to receive in input the differential corrections obtained from a Continuous Operating Reference Stations (CORSs) network.

3 THE TESTS PERFORMED

The experiments using this mass-market receivers for Network Real Time Kinematic (NRTK) positioning were performed within the Regione Piemonte (http://gns.regione.piemonte.it/frmIndex.aspx) CORSs network (Figure 1). The network product used is the VRS[®] stream broadcasted by the network software SpiderNet of the Leica Geosystems[®] Company.

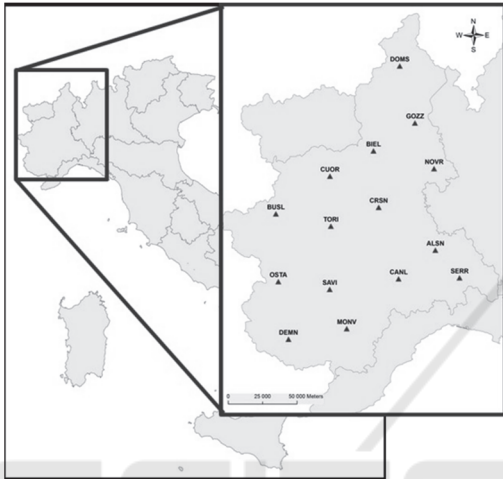


Figure 1: The GNSS CORSs network of Regione Piemonte.

In previous studies (Bellone et al., 2016) it was possible to analyze the performances obtainable considering a static positioning using both real-time and post-processing approaches with this type of receiver and antenna.

The antenna was mounted on a sledge (Figure 2) composed by a complex system of micrometric screws that allow small and controlled displacements, in order to verify the quality of the positioning and the reliability of the statistic tests that were to be performed.

The movements are set by means of a hand-wheel, which moves the sledge along the rail. It is therefore possible with a millimetre tape to obtain direct and visual information about the movements in order to compare the imposed movements against those measured by GNSS instruments. With this sledge, horizontal and vertical movements up to 1.30 m and 0.4 m respectively are possible.

As stated in previous studies (Cina et al., 2014; Bellone et al., 2016), there is always a precision of the sledge movement of about 1mm. Therefore it is possible to consider this value as the “scale resolution” of this support.

The patch antenna was mounted on this sledge as shown in Figure 2. The positioning results were obtained with a frequency of 1 Hz, considering displacements equal to 1 cm both in planimetry and in altimetry which were provided manually at 30 second intervals.



Figure 2: The sledge where the GNSS antenna was mounted.

To perform the NRTK positioning, the routines RTKLIB V. 2.4.2 (http://www.rtklib.com/) were used (Takasu and Yasuda, 2009). This software was chosen because it supports standard and precise positioning algorithms with GPS, Global'naja Navigacionnaja Sputnikovaja Sistema (GLONASS) and Quasi-Zenith Satellite System (QZSS) constellations, considering also different positioning modalities for both real-time and post-processing approaches: single-point, DGPS/DGNSS, Kinematic, Static, Moving-baseline, Fixed, etc. Moreover the software is able to manage both the proprietary messages (e.g. u-blox LEA-4T, 5T, 6T) and external communication via serial, TCP/IP, NTRIP etc. of several GNSS receivers. In particular, the RTKNAVI tool was used for these experiments. This tool allows the input of both the raw data (pseudorange and carrier-phase measurements) of the u-blox receiver and the stream data coming from a network with NTRIP authentication (Weber et al., 2006). For this reason the receiver was connected to a laptop to enable Internet connection and to store the NMEA sentences (Manzino and Dabove, 2013). Another peculiarity of this software is that it allows the fixing of the phase ambiguity for real-time kinematic positioning, even if the receiver uses only the L1 GPS frequency.

4 THE USE OF KALMAN FILTER TO DETECT DISCONTINUITIES

The Kalman Filter (KF) was designed to estimate linear dynamic systems (Kalman, 1960; Kalman and Bucy, 1961). According to Grewal and Andrews (1993), the Kalman Filter is an estimator for what is called the linear-quadratic Gaussian (according to Linear Quadratic Gaussian – LQG) (Mäkilä, 2004), while Maybeck (1979) claims that the Kalman Filter is simply an optimal recursive data processing algorithm.

The intuition of this filter is represented by the possibility of updating an estimate of the least squares adjustment due to the introduction of new observations, without recalculating the entire system.

The Kalman filter consists of two steps (Welch and Bishop, 2003): filtering and smoothing. The first allows the best parameter estimation at the current epoch to be determined, while the second, starting from the last epoch of measurement, allows the best parameter estimation of the previous epochs to be determined. For the real-time purposes of this study, only the filtering process is applicable. Unlike the sequential least squares method, one characteristic of the Kalman filter is represented by the fact that it can be used for dynamic problems (Wei et al., 2010).

For this reason, the vector containing the parameters to be estimated will be called the *state vector*.

This vector, which contains, for example, the position and speed of an aeroplane, is not the same at the time i and at the time $i-1$. It is possible to assume, however, the existence of a simple relationship (e.g. linear), among the state parameters of two following epochs, the said *state equation*:

$$x_{i|i-1} = F_{i-1} \cdot x_{i-1|i-1} + \varepsilon_i \quad (1)$$

where F_{i-1} is the *system transition matrix*, $x_{i|i-1}$ and $x_{i-1|i-1}$ are the *state vectors* at different epochs.

The measurement equation, similar to that commonly used in the least squares method, should now be added:

$$L_i = H_i \cdot x_i + e_i \quad (2)$$

where L_i is the measurement vector and H_i is the observation matrix at epoch i .

As it is possible to see from (1), the state equation includes the errors ε_i , which assumes zero mean and known dispersion matrix $C_{\varepsilon\varepsilon}$. On the other side, the

measurement equation (2) includes the measurement errors e_i , that also, in this case, are assumed to have zero mean and known dispersion matrix C_{ee} . Another hypothesis is given by the fact that it is assumed that the measurement errors are independent with respect to the state errors.

Given these preliminary remarks relating to the classic version of the filter, it is necessary to analyze in which way the measurement and state equations can be modified if there is bias. The first applications dates to Teunissen (1998) and Tiberius (1998) where the goal was the detection and resolution "on the fly" of cycle slips, or rather with a moving receiver. The authors in fact apply to the KF a well-known procedure that has already been previously applied, called DIA. The acronym indicates the three steps of the process: Detection, Identification and Adaptation.

This procedure can also be considered for the detection of movements or displacements, especially if these movements are quick (i.e. occurring within only two epochs), and if the accuracy of the instruments allows their observation.

In this case, equation (1) can be written as

$$x_{i|i-1} = T \cdot x_{i-1|i-1} + B \cdot b_{i-1|i-1} + \varepsilon \quad (3)$$

$$y_{i|i-1} = H \cdot x_{i|i} + C \cdot b_{i|i} + e \quad (4)$$

where x is a vector that identifies the position and the velocity of the point with respect to the initial position while y is a scalar value that represents the difference between the coordinates estimated at epoch i and $i-1$. The b term represents the biases, such that the possible displacements occurred between two consecutive epochs. If one considers only the height component (called z) the relationship can be written as:

$$x = \begin{pmatrix} z \\ v \end{pmatrix} \text{ and } b = \begin{pmatrix} b_z \\ b_v \end{pmatrix} \quad (5)$$

where z is the position and v the velocity of the point (b_z is the bias of the position and b_v the bias of the velocity) considering only the up component. So

$$T = \begin{bmatrix} 1 & \Delta t \\ 0 & 1 \end{bmatrix} \text{ and } B = \begin{bmatrix} 1 & 0 \\ 0 & 1 \end{bmatrix} \quad (6)$$

under the hypothesis of a constant and known velocity motion, x and b become scalar values, then:

$$\xi = \begin{pmatrix} x \\ b \end{pmatrix} = \begin{pmatrix} z \\ v_z \\ b_z \\ b_{v_z} \end{pmatrix} \quad \text{and} \quad A = [H \quad C] \quad (7)$$

$$F = \begin{pmatrix} T & 0 \\ 0 & B \end{pmatrix} = \begin{pmatrix} 1 & \Delta t & 0 & 0 \\ 0 & 1 & 0 & 0 \\ 0 & 0 & 1 & 0 \\ 0 & 0 & 0 & 1 \end{pmatrix}$$

So, equations (1) and (2) can be written as:

$$\begin{aligned} \xi_{i|i-1} &= F \cdot \xi_{i-1|i-1} + w \\ y_{i|i} &= H \cdot \xi_{i|i} + e \end{aligned} \quad (8)$$

with

$$C_{ww} = \begin{bmatrix} I_{2 \times 2} & 0_{2 \times 2} \\ 0_{2 \times 2} & 0_{2 \times 2} \end{bmatrix} \cdot \begin{pmatrix} C_{ee} & 0_{2 \times 2} \\ 0_{2 \times 2} & 0_{2 \times 2} \end{pmatrix}$$

where I (in the first equation) represents the identity matrix and C_{ee} is the var-covariance matrix of parameters. If the mean velocity is set equal to zero, previous equations can be written as:

$$\begin{aligned} \xi &= \begin{bmatrix} x \\ b \end{bmatrix}_{i|i-1} = \begin{bmatrix} z \\ b_z \end{bmatrix}_{i|i-1} = \begin{bmatrix} 1 & 0 \\ 0 & 1 \end{bmatrix} \cdot \begin{bmatrix} z \\ b_z \end{bmatrix}_{i-1|i-1} \\ y_{i|i} &= H \cdot \xi_{i|i} + e_{i|i} = [1 \quad 1] \cdot \begin{bmatrix} x \\ b \end{bmatrix}_{i|i} \end{aligned} \quad (9)$$

The var-covariance matrices in these experiments are chosen respectively as:

$$\begin{aligned} C_{ee} &= \begin{bmatrix} 10^{-5} & 0 \\ 0 & 10^{-3} \end{bmatrix} m^2 \\ C_{ee} &= \begin{bmatrix} 10^{-4} & 0 \\ 0 & 10^{-4} \end{bmatrix} m^2 \end{aligned} \quad (10)$$

The weights were chosen according to both the accuracy of the measurements and the expected displacements (that have an order of magnitude of 1 cm) in an adaptive way.

As it is known, at every period it is possible to test the predicted residuals. If these last are defined as:

$$\hat{v} = (y_i - H_i \cdot \xi_{i|i-1}) \quad (11)$$

with their var-covariance matrix

$$Q_{\hat{v}} = H_i \cdot Q_{i|i} \cdot H_i^T + C_e \quad (12)$$

it is possible to identify the displacement as an outlier, according to the χ^2 test. The $Q_{i|i}$ represents the var-covariance matrix of parameters estimated at epoch i .

Since, in this case, there is only one measurement equation but two unknowns, the DIA does not provide reliable results, as is known in the literature (Baarda, 1968; Teunissen and Salzmann, 1989; Salzmann 1995). However, by using the Kalman filter, the solution can also be obtained in this case.

Accordingly, the Thomson test can be used in order to define if a displacement occurs:

$$w_i = \frac{\hat{v}_i}{\hat{\sigma}_i} \sim \tau_{\alpha, dof} \quad (13)$$

where α represents the significance level (in our case equal to 10 % that represents the probability of rejecting the null hypothesis when it is true) and dof is the degree of freedom of the system, that in this case can be determined as the trace of the redundancy matrix R

$$dof = tr(R) = tr(I - H \cdot Q_{i|i} \cdot H^T \cdot C_{ee}^{-1}) \quad (14)$$

So if $w_i < \tau_{\alpha, dof}$ it can be assumed that the obtained values are the positioning results, otherwise there is the possibility that a displacement occurs. In this case, if $w_i \geq \tau_{\alpha, dof}$ the Minimum Detectable Bias (MDB) is calculated in order to verify if this value is a real displacement.

5 DATA PROCESSING AND RESULTS COMPARED WITH OTHER METHODS

The method previously described is applied to two real-time datasets that simulates a landslide. As previously stated, the system was composed as shown in Figure 2. The positioning results were obtained with a frequency of 1 Hz, considering displacements equal to 1 cm both in planimetry and in altimetry provided manually every 30 seconds. This can be seen in Figure 4, where two cases, one with good (number of satellites greater than 7) and another one with low (only 5 satellites) satellite visibility, are considered. The results shown in this paper will refer only to the second case, that represents the worst available possibility.

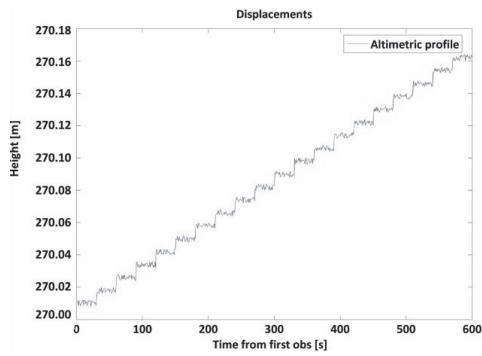


Figure 3: Altimetric profile of displacements with good (more than 7 satellites - left) satellite visibility.

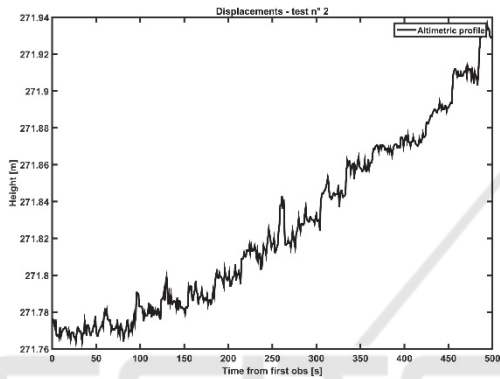


Figure 4: Altimetric profile of displacements with poor (only 5 satellites - right) satellite visibility.

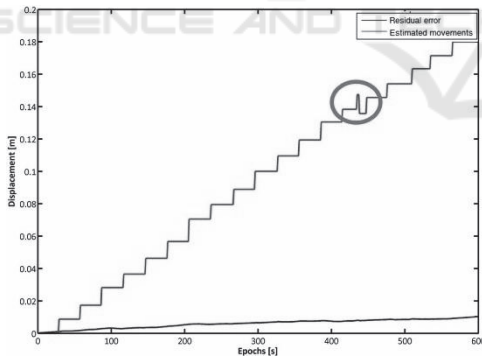


Figure 5: Planimetric trend (up) and estimated bias (down).

The goal is to estimate the most probable value of the bias (the occurred shift) and to add it to the value of the bias of the previous period.

As it is possible to see from Figure 5, despite some errors in the estimation of discontinuities (in the circle), the solution seems to be correct. If the detected displacements are analyzed, a success rate of 96.1% is obtained (i.e. real displacements detected correctly). As well, 1.3% of undetected displacements (i.e. real displacements not detected) and 2.6% of

false alarms (it means that the filter has declared a displacement that it has not occurred) are identified. An example of undetected or correctly detected displacements can be seen in Figure 7, where also a summary of obtained results can be found. Must to be underlined that no significant differences in terms of success rate can be obtained according to the number of visible satellites, even if the quality of the positioning changes as it is possible to see from Figure 3. The reported tests were made considering from 5 up to 7 satellites while all results shown in this work are obtained with a number of satellites equal to 6, that is a reasonable number of satellites visible with mass-market receivers, also in hard-environment conditions.

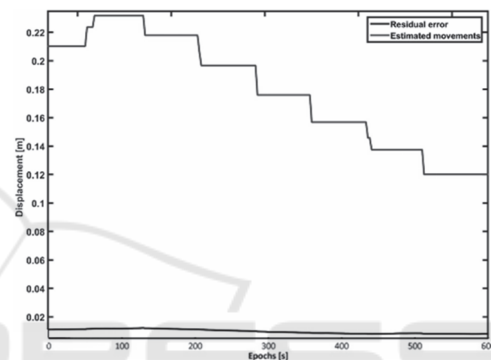


Figure 6: Altimetric trend (up) and estimated bias (down).

Also the root mean square (RMS) values of the solution and biases are evaluated. As can be seen from Figure 8, the accuracy of the solution is very high. This means that the Kalman filter can be considered as a useful tool to detect displacements with this type of receivers and that the tuning of the filter was correctly achieved.

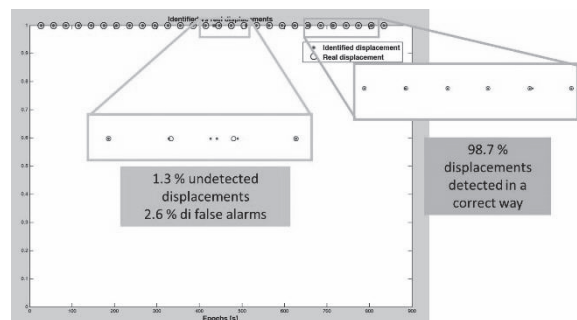


Figure 7: Results obtained with the Kalman filter.

If the tuning is carried out correctly, this filter allows both to decrease the accidental error of RTK positioning and to control the possible gross-errors or outliers that can be due to a false fix of the phase

ambiguity and not to an unexpected displacement (in this case this error goes to zero at the next epoch).

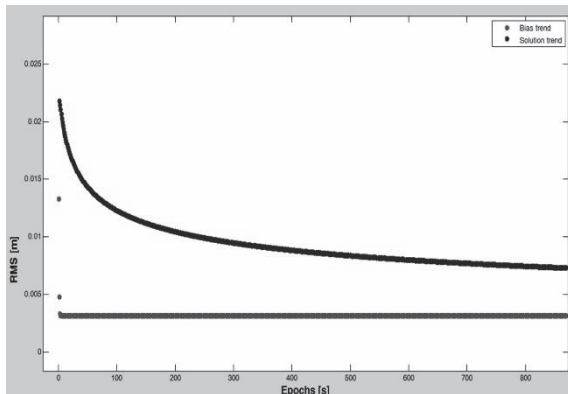


Figure 8: RMS of estimated biases and solution.

This can be affirmed considering the previous results (Figure 8) and those obtained if a planimetric positioning error of 24 hours is considered (Figure 9).

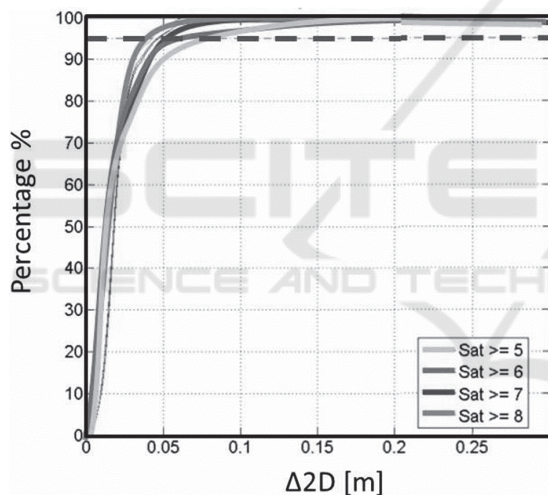


Figure 9: Planimetric positioning error (the dotted line represents the significance level equal to 95%).

In fact, in the first case the RMS of positioning (less than 2 cm) is better than those obtained in the following graph (5 cm at 95% of reliability).

Finally, these results were compared with those obtained in a previous study based on a modified Chow test. Applying the methods described in the literature (Bellone et al., 2016), and considering a 10-element sample size (meaning that a sample composed of 10 epochs = 10 seconds of latency of alarm at 1 Hz of acquisition rate), this method correctly identified 93.1% of the displacements, with a very low rate of false alarms equal to 3.3%. Anyway these values are greater than those estimated with the

Kalman filter, that has shown the best performances in terms of both false alarms (2.6%) and undetected displacements (1.3%).

6 CONCLUSIONS

In this study, the Kalman filtering technique has been applied for kinematic deformation analysis procedure. A GPS data set that simulates a landslide movement was collected and the proposed method has been tested. The two methods (Kalman filter and modified Chow test) produced comparable results, even though the proposed version of the Kalman filter has shown the best performance. Interesting results have been obtained in real-time also by employing a mass-market GPS receiver. In this context, the results have shown the possibility of using this type of receivers for this kind of application.

The employment of these receivers on a landslide site could be useful also from an economic point of view. The total cost of receiver, antenna, transmission system and power supply (solar panel and battery) is about € 600. The advantage is that the economic damage in case of an unexpected event is less than could occur if a geodetic GNSS instrumentation is utilized. At the same time, it is possible to calculate the position of the receivers in a similar way to the CORS network, with obvious advantages in the precision and accuracy of the results and the landslide analysis.

This study has considered static motion but it is also possible to suppose a motion where the bias is the change of velocity between two points.

Considering some preliminary results, in this last case the Kalman filter appears to provide better results with respect to statistical tests. This aspect will be investigated subsequently.

REFERENCES

- Aharizad, N., Setan, H., Lim, M. 2012. Optimized Kalman filter versus rigorous method in deformation analysis. *Journal of Applied Geodesy*, 6(3-4), 135-142.
- Acar, M., Özlüdemir, M. T., Çelik, R. N., Erol, S., Ayan, T. 2004. "Landslide monitoring through kalman filtering: A case study in Gürpınar". *Proceeding of XXth ISPRS Congress, Istanbul, Turkey*.
- Baarda, W. 1968. A Testing Procedure for Use in Geodetic Networks. Netherlands Geodetic Commission. *Publications on Geodesy - New Series*. Vol. 2. No. 5.
- Bellone, T., Dabove, P., Manzano, A.M., Taglioretti, C. 2016. Real-time monitoring for fast deformations using GNSS low-cost receivers. *Geomatics, Natural Hazards*

- and Risk, 7(2):458-470. Available at: <http://dx.doi.org/10.1080/19475705.2014.966867>.
- Benoit, L., Briole, P., Martin, O., Thom, C. 2014. Real-time deformation monitoring by a wireless network of low-cost GPS. *Journal of Applied Geodesy*, 1-10.
- Bertachini, E., Capitani, A., Capra, A., Castagnetti, C., Corsini, A., Dubbini, M., Ronchetti, F. 2009. Integrated surveying system for landslide monitoring, Valoria landslide (Appennines of Modena, Italy). Paper presented at: *FIG working week 2009*, Eilat, Israel.
- Brückl, E., Brunner, F.K., Lang, E., Mertl, S., Müller, M., Stary, U. 2013. The Gradenbach Observatory - monitoring deep-seated gravitational slope deformation by geodetic, hydrological, and seismological methods. *Landslides* 10 (2013): 815 – 829.
- Calcaterra, S., Cesi, C., Di Maio, C., Gambino, P., Merli, K., Vallario, M., Vassallo, R. 2012. Surface displacements of two landslides evaluated by GPS and inclinometer systems: a case study in Southern Appennines, Italy. *Nat Hazards* 61(1):257–266.
- Chrzanowski, A., Chen, Y., Romero, P. and Secord, J.M. 1986. Integration of Geodetic and Geotechnical Deformation Surveys in the Geosciences. *Tectonophysics*, Vol. 130, No. 1-4, November: 369-383.
- Chow, G. C. 1960. Tests of Equality Between Sets of Coefficients in Two Linear Regressions. *Econometrica* 28(3): 591–605.
- Cina, A., Piras, M. 2014. Monitoring of landslides with mass market GPS: an alternative low cost solution. *Geomatics, Natural Hazards and Risk*. [cited 2014 Feb 24]. Available from: <http://www.tandfonline.com/doi/full/10.1080/19475705.2014.889046#U0-vV6IzfcB>.
- Coe, J.A., Ellis, W.L., Godt, J.W., Savage, W.Z., Savage, J.E., Michael, J.A., Kibler, J.D., Powers, P.S., Lidke, D.J., Debray, S. 2003. Seasonal movement of the Slumgullion landslide determined from Global Positioning System surveys and field instrumentation, July 1998-March 2002. *Engineering Geology*, 68 (1–2): 67–101.
- Cruden, D.M. 1991. A simple definition of a landslide. Bulletin of the international association of engineering geology. *Bulletin de l'Association Internationale de Géologie de l'Ingénieur*. 43(1):27–29.
- Dabove, P., Manzino, A.M., Taglioretti, C. 2014. GNSS network products for post-processing positioning: limitations and peculiarities. *Applied Geomatics*, vol. 6 n. 1, pp. 27-36. - ISSN 1866-9298. Available at: <http://link.springer.com/article/10.1007/s12518-014-0122-3>.
- Dabove, P., Manzino, A.M. 2014. GPS & GLONASS Mass-Market Receivers: Positioning Performances and Peculiarities. *Sensors* 2014, 14, 22159-22179.
- Eyo Etim, E., Tajul, A.M., Khairulnizam, M.I., Yusuf, D.O. 2014. Reverse RTK Data Streaming for Low-Cost Landslide Monitoring. *Geoinformation for Informed Decisions. Lecture Notes in Geoinformation and Cartography*. Springer International Publishing, Switzerland.
- Gili, J.A., Corominas, J., Rius, J. 2000. Using global positioning system techniques in landslide monitoring. *Eng Geol* 55(3):167–192.
- Günther, J., Heunecke, O., Pink, S., Schuhbäck, S. 2008. Developments towards a low cost GNSS Based Sensor Network for the monitoring of landslides. Paper presented at: *13th FIG International Symposium on Deformation Measurements and Analysis*, Lisbon.
- Gülal, E. 1999. Application of Kalman filtering technique in the analysis of deformation measurements. *Journal of Yildiz Technical University*, (1). (in Turkish).
- Hastaoglu, K.O., Sanli, D.U. 2011. Monitoring Koyulhisar landslide using rapid static GPS: a strategy to remove biases from vertical velocities. *Natural Hazards*. 58:1275-1294.
- Heunecke, O., Glabsch, J., Schuhbäck, S. 2011. Landslide Monitoring Using Low Cost GNSS Equipment – Experiences from Two Alpine Testing Sites. *Journal of Civil Engineering and Architecture*. 45:661-669.
- Janssen, V., & Rizos, C. (2003). A mixed-mode GPS network processing approach for deformation monitoring applications. *Survey review*, 37(287), 2-19.
- Kalman, R.E. 1960. A new approach to linear filtering and prediction problems. *Trans. ASME J. Basic Engr*: 35-45.
- Li, L., Kuhlmann, H. 2008. Detection of deformations and outliers in Real-time GPS measurements by Kalman Filter Model with Shaping Filter. In: *4th IAG Symposium on Geodesy for Geotechnical and Structural Engineering and 13th FIG Symposium on Deformation Measurements*, Lisbon.
- Li, L., Kuhlmann, H. 2010. Deformation Detection in the GPS Real-time Series by the Multiple Kalman Filter Model. *Journal of Surveying Engineering*. 136:157-164.
- Li, L., Kuhlmann, H. 2012. Real-time deformation measurements using time series of GPS coordinates processed by Kalman filter with shaping filter. *Survey Review*, Vol. 44, 326:189-197.
- Mäkilä, P.M. 2004. Kalman Filtering and Linear Quadratic Gaussian Control. *Lecture notes for course 7604120*, Part I. Available at: http://www.dt.fee.unicamp.br/~jbosco/ia856/KF_part1_Makila.pdf.
- Malet, J-P., Maquaire, O., Calais, E. 2002. The use of global positioning system techniques for the continuous monitoring of landslides: application to the super-sauze earth flow (Alpes-de-Haute-Provence, France). *Geomorphology* 43:33–54.
- Manzino, A.M., Dabove, P. 2013. Quality control of the NRTK positioning with mass-market receivers. *Global Positioning Systems: Signal Structure, Applications and Sources of Error and Biases*. Ya-Hui Hsueh, Hauppauge NY. Chapter 2. p. 17-40.
- Masiero, A., Guarnieri, A., Vettore, A., Pirotti, F. 2013. A nonlinear filtering approach for smartphone-based indoor navigation. May 2013, 1-3, Tainan, Taiwan.
- Mora, P., Baldi, P., Casula, G., Fabris, M., Ghirotti, M., Mazzini, E., Pesci, A. 2003. Global positioning systems

- and digital photogrammetry for the monitoring of mass movements: application to the Ca' di Malta landslide (northern Apennines, Italy). *Eng Geol* 68(1–2):103–121.
- Moss, J.L. 2000. Using the global positioning system to monitor dynamic ground deformation networks on potentially active landslides. *Int J Appl Earth Obs Geoinf*, 2(1):24–32.
- Othman, Z., Wan Aziz, W.A., Anuar, A. 2011. Evaluating the performance of GPS survey methods for landslide monitoring at hillside residential area: static vs rapid static. *IEEE 7th international colloquium on signal processing and its applications*, George Town, Penang.
- Peyret, M., Djamour, Y., Rizza, M., Ritz, J. F., Hurtrez, J.E., Goudarzi, M.A., Nankali, H., Chery, J., Le Dortz, K., Uri, F. 2008. Monitoring of the large slow Kahrod landslide in Alboz mountain range (Iran) by GPS and SAR interferometry. *Eng. Geol.* 100:131-141.
- Rizzo, V. 2002. GPS monitoring and new data on slope movements in the Maratea Valley (Potenza, Basilicata). *Phys Chem Earth, Parts A/B/C* 27(36):1535–1544.
- Rott, H., Nagler, T. 2006. The contribution of radar interferometry to the assessment of landslide hazards. *Adv Space Res* 37(4):710–719.
- Salzmann, M.A. 1995. Real-time adaptation for model errors in dynamic systems. *Bulletin Geodesique*, 69:81–91.
- Sedlak, V., Jecny, M. 2004. Deformation measurements on Bulk Dam of waterwork in East Slovakia. *Geology, Ecology, Mining Service*, Vol. L, No. 2, 1-10.
- Szostak-Chrzanowski, A., Chrzanowski, A., & Massiera, M. (2005). Use of deformation monitoring results in solving geomechanical problems—case studies. *Engineering Geology*, 79(1), 3-12.
- Tagliavini, F., Mantovani, M., Marcato, G., Pasuto, A., Silvano, S. 2007. Validation of landslide hazard assessment by means of GPS monitoring technique – a case study in the Dolomites (Eastern Alps, Italy). *Nat. Hazards Earth Syst. Sci.*, 7:185-193,
- Takasu, T., Yasuda, A. 2009. Development of the low-cost RTK GPS receiver with the open source program package RTKLIB. *International symposium on GPS/GNSS, International convention centre, Jeju, Korea.*
- Teunissen, P.J.G., Salzmann, M.A. 1989. A recursive slip-page test for use in state-space filtering. *Manuscripta Geodaetica*, 14:383-390.
- Wang, G. 2011. GPS landslide monitoring: single base vs. network solutions—a case study based on the Puerto Rico and Virgin Islands permanent GPS network. *J Geodetic Sci* 1(3):191–203.
- Wang, G., Soler, T. 2012. OPUS for horizontal sub-centimeter accuracy landslide monitoring: case study in Puerto Rico and Virgin Islands region. *J Surv Eng* 138(3):11.
- Weber, G., Dettmering, D., Gebhard, H. 2006. Networked transport of RTCM via internet protocol (NTRIP). *International association of geodesy symposia: a window on the future of geodesy*, vol 128.
- Welch, G., Bishop, G. 2003. An introduction to the Kalman Filter. *TR95-04*, Department of Computer Science, University of North Carolina at Chapel Hill. Available at: <http://citeseerx.ist.psu.edu/viewdoc/download?doi=10.1.1.117.6808&rep=rep1&type=pdf>.
- Welsch, W., Heunecke, O. (2001). Models and terminology for the analysis of geodetic monitoring observations. *Official report of the ad-hoc committee of FIG working group*, 6, 390-412.
- Wei, Z., Dongli, F., Jinzhong, Y. 2010. Adaptive Kalman Filtering Method to the Data Processing of GPS Deformation Monitoring. *Proceedings of the 2010 International Forum on Information Technology and Applications - Volume 01 (IFITA '10)*, Vol. 1. IEEE Computer Society, Washington, DC, USA, 288-292. DOI=10.1109/IFITA.2010.18 <http://dx.doi.org/10.1109/IFITA.2010.18>.